BIT Numerical Mathematics (2025) 65:44
https://doi.org/10.1007/s10543-025-01087-4

BIT

Error analysis of Gauss quadrature approximation to hypergeometric functions

Eleonora Denich[1] · **Paolo Novati**[1]

Received: 26 May 2025 / Accepted: 17 October 2025

Abstract

Exploiting the contour integral representation of the remainder term in Gaussian quadrature, in this work we derive explicit error approximations for the computation of the confluent and the Gauss hypergeometric functions by means of the Gauss-Jacobi rule. Some numerical examples illustrate the quality of the estimates.

Keywords Hypergeometric functions · Gauss-Jacobi rule · Contour integral representation · Asymptotic analysis

Mathematics Subject Classification 33C05 · 33C15 · 30E15 · 65D32

1 Introduction

The computation of the confluent and Gauss hypergeometric functions is a classical topic in the field of the numerical approximation of special functions. The confluent hypergeometric function (Kummer's function) is a generalized hypergeometric series given by (see [1, 13.4.1])

$$M(a, b, z) = \sum_{n=0}^{\infty} \frac{(a)_n z^n}{(b)_n n!},$$

where

$$(a)_n = \begin{cases} 1, & n = 0 \\ a(a+1)(a+2)\dots(a+n-1), & n > 0 \end{cases}$$

Eleonora Denich and Paolo Novati contributed equally to this work.

✉ Eleonora Denich
eleonora.denich@units.it

Paolo Novati
novati@units.it

1 Department of Mathematics, Informatics and Geosciences, University of Trieste, Via Valerio 12/1, 34127 Trieste, Italy

Published online: 27 October 2025

is the rising factorial. On the other hand, the Gauss hypergeometric function is defined by the series (see [1, 15.6.1])

$$F(a,b,c,z) = \sum_{n=0}^{\infty} \frac{(a)_n (b)_n z^n}{(c)_n n!},$$

for $|z| < 1$, and by analytic continuation elsewhere. Among the existing methods commonly used for these particular hypergeometric functions (see [2] and the reference therein for a comprehensive background), in this work we consider the method based on the Gauss-Jacobi quadrature, discussed by W. Gautschi in [3]. The use of this rule seems natural and attractive whenever the parameters and the arguments of the hypergeometric functions allow the following integral representations, in which the Jacobi weight explicitly appears (see [1, 13.4.1 and 15.6.1]):

$$M(a,b,z) = \frac{1}{\Gamma(a)\Gamma(b-a)} \int_0^1 e^{zt} t^{a-1} (1-t)^{b-a-1} dt, \quad \text{for} \quad b > a > 0, \tag{1}$$

where $\Gamma(\cdot)$ denotes the Gamma function, and

$$F(a,b,c,z) = \frac{1}{\Gamma(b)\Gamma(c-b)} \int_0^1 \frac{t^{b-1}(1-t)^{c-b-1}}{(1-zt)^a} dt, \tag{2}$$

for $|\arg(1-z)| < \pi, \ c > b > 0$.

In this paper we do not introduce new methods but revisit the error analysis presented in [3], with the basic aim of providing reliable and easy to use error estimates. In particular, we derive explicit formulas in terms of the number of quadrature points, the parameters and the argument of the hypergeometric functions. These estimates are rather accurate for a reasonable range of values of the parameters and, therefore, may represent a useful tool for automatic computation with prescribed accuracy. The analysis is based on the theory of analytic functions (see e.g. [4, section 4.6] for an overview) and makes use of the Cauchy integral representation of the remainder term of the quadrature rule.

In this work the symbols $\sim$ and $\lesssim$ stand for asymptotically equal and less than or asymptotically equal to, respectively.

The paper is organized as follows. In Section 2 we briefly recall the Gauss-Jacobi rule, together with the integral representation of the remainder term, and give some technical results. Sections 3 and 4 deal with the error analysis of the Jacobi rule for the computation of the confluent and the Gauss hypergeometric function, respectively. In Section 5 we test the error estimates on some examples.

2 Background and preliminary results

Given

$$w_{\alpha,\beta}(t) = (1-t)^{\alpha}(1+t)^{\beta}, \quad t \in (-1,1), \ \text{for } \alpha, \beta > -1,$$

and a generic function f, for the computation of

$$I^{\alpha,\beta}(f) = \int_{-1}^{1} f(t) w_{\alpha,\beta}(t) dt$$

the n-point Gauss-Jacobi quadrature rule reads

$$I_n^{(\alpha,\beta)}(f) = \sum_{j=1}^{n} \lambda_j f(t_j), \tag{3}$$

where t_j and λ_j, $j = 1, \ldots, n$, are the Gauss-Jacobi nodes and weights. It is well known that t_j and λ_j can be expressed in terms of the spectral data of the associated Jacobi matrix [5]. As for the remainder

$$\mathcal{R}_n(f) = I^{(\alpha,\beta)}(f) - I_n^{(\alpha,\beta)}(f),$$

by means of the Cauchy formula, it can be written as (see [6])

$$\mathcal{R}_n(f) = \frac{1}{2\pi i} \int_{\mathcal{C}} K_n(w) f(w) dw, \tag{4}$$

where the contour $\mathcal{C}$ contains in its interior the interval of integration $[-1, 1]$ but no singularity of the function f lies on or within the contour. In the above formula the kernel K_n is given by

$$K_n(w) = \frac{\pi_n^{(\alpha,\beta)}(w)}{P_n^{(\alpha,\beta)}(w)},$$

where $P_n^{(\alpha,\beta)}$ is the Jacobi polynomial of degree n and

$$\pi_n^{(\alpha,\beta)}(w) = \int_{-1}^{1} \frac{w_{\alpha,\beta}(t) P_n^{(\alpha,\beta)}(t)}{w - t} dt$$

is known as the associated Jacobi function (see [4, section 1.12]). In particular, for $n \to +\infty$ and w not in the neighborhood of $[-1, 1]$ it holds (cf. [7])

$$|K_n(w)| \sim 2\pi \, |w - 1|^{\alpha} \, |w + 1|^{\beta} \left| w + (w^2 - 1)^{1/2} \right|^{-2n-\alpha-\beta-1}. \tag{5}$$

For $r > 1$ and $0 \le \theta < 2\pi$, we introduce the function

$$\psi(re^{i\theta}) = \frac{1}{2} \left(re^{i\theta} + \frac{1}{re^{i\theta}} \right), \tag{6}$$

that allows to define the family of confocal ellipses

$$\Gamma_r = \left\{ w \in \mathbb{C} \mid w = \psi(re^{i\theta}),\ 0 \le \theta < 2\pi \right\}, \tag{7}$$

having foci at ± 1 and the sum of semiaxis equal to r. We observe that $\left|w+(w^2-1)^{1/2}\right| = r$ on any particular ellipse of type (7). Let $r_p > 1$ be the smallest real number such that a singularity of f, named p, is on Γ_{r_p}. In this situation, the standard approach consists in taking Γ_r, $1 < r < r_p$, as contour in (4), so that the remainder term can be bounded as (see (5))

$$\begin{aligned} |\mathcal{R}_n(f)| &\leq \frac{1}{2\pi} \max_{w \in \Gamma_r} |f(w)| \int_{\Gamma_r} |K_n(w)||dw| \\ &\lesssim C_{\alpha,\beta}(r) r^{-2n-\alpha-\beta-1} \max_{w \in \Gamma_r} |f(w)|, \end{aligned} \tag{8}$$

where

$$C_{\alpha,\beta}(r) = \int_{\Gamma_r} |w-1|^{\alpha} \, |w+1|^{\beta} \, |dw|. \tag{9}$$

As we will see in Sect. 3, the function f, that appears in the integral representation of the confluent hypergeometric function, is entire. In this case formula (8) holds true $\forall r > 1$, and one needs to optimize the bound with respect to r. Typically, because of (5), the optimal value grows with n. In this view, since

$$C_{\alpha,\beta}(r) \leq \ell(\Gamma_r) \max_{w \in \Gamma_r} |w-1|^{\alpha} \, |w+1|^{\beta} \, ,$$

where $\ell(\Gamma_r)$ denotes the length of the ellipse Γ_r, we can write

$$\begin{aligned} &\max_{w \in \Gamma_r} |w-1|^{\alpha} \, |w+1|^{\beta} \\ &= \max_{\theta \in [0,2\pi]} \left| \left(\frac{1}{2} \left(re^{i\theta} + \frac{1}{re^{i\theta}} \right) - 1 \right)^{\alpha} \left(\frac{1}{2} \left(re^{i\theta} + \frac{1}{re^{i\theta}} \right) + 1 \right)^{\beta} \right| \\ &= \max_{\theta \in [0,2\pi]} \frac{|(re^{i\theta}-1)^{2\alpha}(re^{i\theta}+1)^{2\beta}|}{(2r)^{\alpha+\beta}} \\ &\sim 2^{-\alpha-\beta} r^{\alpha+\beta}, \quad r \to +\infty. \end{aligned}$$

Moreover, since for $r \to +\infty$, $\ell(\Gamma_r) \sim 2\pi r$, we obtain

$$C_{\alpha,\beta}(r) \lesssim 2^{1-\alpha-\beta} \pi r^{\alpha+\beta+1}. \tag{10}$$

This approach will be used for the confluent hypergeometric function in Sect. 3. In the case of the Gauss hypergeometric function, the properties of the corresponding function f are such that the optimization of (8) with respect to $1 < r < r_p$ leads to error estimates not very sharp. This strategy has been used in [3], where the optimal r is numerically evaluated. In Sect. 4 we introduce a different approach, that allows to obtain more reliable approximations.

3 Confluent hypergeometric function

For $b > a > 0$ and $z \in \mathbb{C}$, the confluent hypergeometric function can be written as (see (1))

$$M(a,b,z) = \frac{1}{\gamma_0^{(a,b)}} \int_{-1}^{1} e^{\frac{1}{2}z(1+t)} w_{b-a-1,a-1}(t)dt,$$

in which

$$w_{b-a-1,a-1}(t) = (1-t)^{b-a-1}(1+t)^{a-1},$$

and

$$\gamma_0^{(a,b)} = \int_{-1}^{1} w_{b-a-1,a-1}(t)dt = 2^{b-1}\frac{\Gamma(b-a)\Gamma(a)}{\Gamma(b)},$$

see [8, 7.391(1)]. Denoting by

$$f_z(t) = e^{\frac{1}{2}z(1+t)}, \tag{11}$$

the n-point Gauss-Jacobi rule (3) leads to

$$M(a,b,z) = \frac{1}{\gamma_0^{(a,b)}} \left(I_n^{(b-a-1,a-1)}(f_z) + \mathcal{R}_n(f_z) \right). \tag{12}$$

In this situation, since f_z is an entire function, for the remainder term we can use formulas (8)-(10) to obtain

$$|\mathcal{R}_n(f)| \lesssim 2^{3-b}\pi \max_{w\in\Gamma_r} |f_z(w)| r^{-2n}, \quad r \to +\infty. \tag{13}$$

As for the maximum of $|f_z(w)|$, we first set $z = \rho e^{i\varphi}$, $\rho > 0$. Then, by (6),

$$\begin{aligned}
\max_{w\in\Gamma_r} |f_z(w)| &= \max_{w\in\Gamma_r} |e^{\frac{1}{2}z(1+w)}| \\
&= \max_{\theta\in[0,2\pi]} |e^{\frac{1}{2}z(1+\psi(re^{i\theta})}| \\
&= \max_{\theta\in[0,2\pi]} e^{\frac{\rho}{2}G(\theta)},
\end{aligned}$$

where

$$G(\theta) = \cos\varphi\left(1 + \frac{1}{2}\cos\theta\left(r + \frac{1}{r}\right)\right) - \sin\varphi\left(\frac{1}{2}\sin\theta\left(r - \frac{1}{r}\right)\right). \tag{14}$$

By imposing $G'(\theta) = 0$ and defining $r_+ = r + \frac{1}{r}$ and $r_- = r - \frac{1}{r}$, we obtain the equation

$$\tan\theta = -\frac{r_-}{r_+}\tan\varphi, \tag{15}$$

valid for $\cos\varphi \neq 0$. Let $\theta^\star = \arg\max_{\theta\in[0,2\pi]} G(\theta)$. We observe that, if $\varphi = \frac{\pi}{2}$, then $\theta^\star = \frac{3}{2}\pi$, and if $\varphi = \frac{3}{2}\pi$, then $\theta^\star = \frac{\pi}{2}$. On the other side, for $\cos\varphi \neq 0$, the solutions of equation (15) are given by the set

$$\theta_k = -\arctan\left(\frac{r_-}{r_+}\tan\varphi\right) + k\pi, \quad k \in \mathbb{Z}.$$

Then, looking for the solution in $[0, 2\pi]$, we find

$$\theta^\star = \begin{cases} \theta_0 & \text{if} \quad 0 \leq \varphi < \frac{\pi}{2} \quad \text{or} \quad \frac{3}{2}\pi < \varphi \leq 2\pi \\ \theta_1 & \text{if} \quad \frac{\pi}{2} < \varphi \leq \pi \\ \theta_{-1} & \text{if} \quad \pi < \varphi < \frac{3}{2}\pi \end{cases}.$$

Inserting the above results in (14) and using classical trigonometric identities, leads to

$$\max_{w\in\Gamma_r} |f_z(w)| = e^{\frac{\rho}{2}\left(\cos\varphi + \sqrt{\left(\frac{r_-}{2}\right)^2 + \cos^2\varphi}\right)} =: \Phi(r),$$

and therefore, by (13), for $r \to +\infty$ we obtain

$$|\mathcal{R}_n(f_z)| \lesssim 2^{3-b}\pi\,\Phi(r) r^{-2n}. \tag{16}$$

At this point, looking for

$$r_n := \arg\min_{r>1} \Phi(r) r^{-2n},$$

we find

$$r_n = \frac{\sqrt{B(n)} + \sqrt{B(n)+4}}{2}, \tag{17}$$

where

$$B(n) = \frac{2\left(16n^2 - \rho^2 + \sqrt{(16n^2-\rho^2)^2 + 64n^2\rho^2\cos^2\varphi}\right)}{\rho^2}. \tag{18}$$

Denoting by $\varepsilon_n^{(a,b)}(z)$ the error of the method (12), that is,

$$\varepsilon_n^{(a,b)}(z) = \left| M(a,b,z) - \frac{I_n^{(b-a-1,a-1)}(f_z)}{\gamma_0^{(a,b)}} \right| = \frac{|\mathcal{R}_n(f_z)|}{\gamma_0^{(a,b)}},$$

by inserting (17) in (16), we finally obtain

$$\varepsilon_n^{(a,b)}(z) \lesssim \frac{2^{3-b}}{\gamma_0^{(a,b)}} \pi\, e^{\frac{\rho}{2}\left(\cos\varphi + \sqrt{\frac{16n^2}{\rho^2} + \cos^2\varphi}\right)} r_n^{-2n}. \tag{19}$$

In order to highlight the asymptotic behavior, we observe that

$$B(n) \sim \frac{64n^2}{\rho^2}, \quad n \to +\infty,$$

which means that r_n grows linearly with n, and therefore

$$\varepsilon_n^{(a,b)}(z) \lesssim \frac{2^{3-b}}{\gamma_0^{(a,b)}}\pi e^{\frac{\rho}{2}\left(\cos\varphi+\frac{4n}{\rho}\right)}\left(\sqrt{B(n)}\right)^{-2n}$$
$$\sim \frac{2^{3-b}}{\gamma_0^{(a,b)}}\pi e^{\frac{\rho}{2}\cos\varphi}\left(\frac{8n}{e\rho}\right)^{-2n}, \quad n \to +\infty. \tag{20}$$

Formula (20) is very similar to the one given in [3, (1.7)], obtained using derivatives. The improvement, anyway, is obtained by employing (19), especially for large $|z|$, $z \in \mathbb{R}$, as we will see in Sect. 5.

4 Gauss hypergeometric function

For $a \in \mathbb{R}$ and $c > b > 0$, the Gauss hypergeometric function can be written as (see (2))

$$F(a,b,c,z) = \frac{1}{\gamma_0^{(b,c)}}\int_{-1}^{1} g_z(t)w_{c-b-1,b-1}(t)dt,$$

where

$$g_z(t) = \left(1 - \frac{1}{2}z(1+t)\right)^{-a}, \quad z \notin [1,+\infty), \tag{21}$$

and

$$\gamma_0^{(b,c)} = 2^{c-1}\frac{\Gamma(c-b)\Gamma(b)}{\Gamma(c)}.$$

The case of a non positive integer is of little interest, since $F(a,b,c,z)$ reduces to a finite sum, that is,

$$F(-m,b,c,z) = \sum_{j=0}^{m}(-1)^j\binom{m}{j}\frac{(b)_j}{(c)_j}z^j, \quad m \in \mathbb{N}.$$

In what follows we therefore assume $a \in \mathbb{R}\setminus\mathbb{Z}^-$. Writing $z = \rho e^{i\varphi}$, $\rho > 0$, the function g_z is analytic, in the variable t, in the whole complex plane cut along the line

$$t = \frac{2(x+1)}{\rho}e^{-i\varphi} - 1, \quad x \in \mathbb{R}^+, \tag{22}$$

with branch point at $p = \frac{2}{z} - 1$. Clearly p is just a pole of order a if $a \in \mathbb{Z}^+$. Anyway we do not need to distinguish these two cases since the following analysis perfectly suits both situations. The method based on the n-point Gauss-Jacobi rule reads

$$F(a,b,c,z) = \frac{1}{\gamma_0^{(b,c)}}\left(I_n^{(c-b-1,b-1)}(g_z) + \mathcal{R}_n(g_z)\right). \tag{23}$$

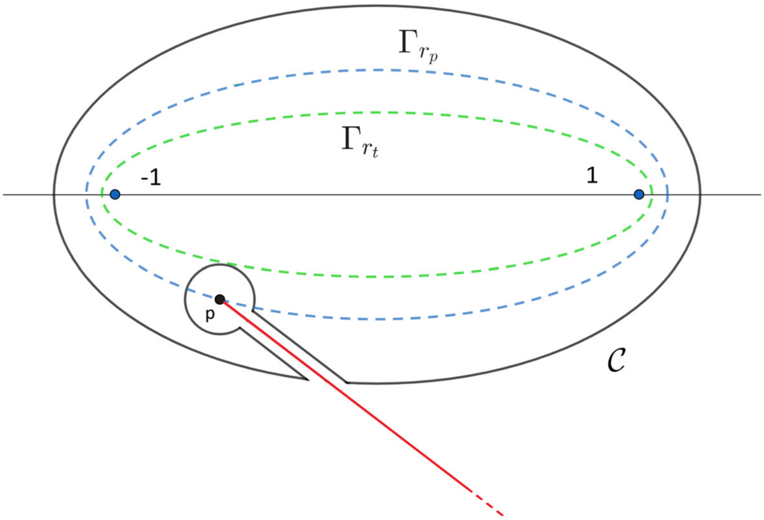

Fig. 1 The contour $\mathcal{C} = C_\delta \cup \ell_1 \cup \ell_2 \cup \Gamma_R$ (black line), the ellipse Γ_{r_p} (dashed blue line) passing through the branch point p, and the ellipse Γ_{r_t} (dashed green line) tangent to the disk $\mathcal{C}_\delta$. In red the branch cut (color figure online)

In order to derive an estimate for the remainder, we first observe that the extension of the cut (22) passes through the point -1, and therefore, the smallest ellipse of the family (7) encountering a singularity, is exactly the one passing through p. In other words, this ellipse is defined by

$$r_p = \left| p + u\sqrt{p^2 - 1} \right|, \tag{24}$$

in which $u = \pm 1$ needs to be selected in order to have $r_p > 1$. In particular, it can be verified that the correct choice is

$$u = \text{sign}\left(\Re\left(\frac{p}{\sqrt{p^2-1}}\right)\right).$$

Note that $p^2 - 1 = 0$ only for $z = 1, +\infty$, where the integral representation does not hold. In this situation, as contour $\mathcal{C}$ in (4) we consider the one depicted in Figure 1, that is, $\mathcal{C} = C_\delta \cup \ell_1 \cup \ell_2 \cup \Gamma_R$, where C_δ is the disk centered at p and with radius δ, $R > r_p$, and ℓ_1, ℓ_2, are the line segments arbitrarily close to the cut that join the ellipse to the circle. In particular, we take $\delta := |p|s$, where s must be small enough in order that the circle does not encounter the interval $[-1, 1]$, nor the ellipse Γ_R.

Looking at Figure 1, it is clear that

$$\min_{w \in \mathcal{C}} \left| w + \sqrt{w^2 - 1} \right| = r_t, \tag{25}$$

where $r_t < r_p < R$ is such that the corresponding Γ_{r_t} is the ellipse tangent to the circle. Even if not explicitly expressed, r_t depends on s. Because of (25) and the asymptotic (5), we can therefore consider the approximation

$$|\mathcal{R}_n(g_z)| \lesssim \frac{1}{2\pi} \int_{C_\delta} |K_n(w) g_z(w) dw|, \quad n \to +\infty,$$

in which we neglect the contribution along the line segments ℓ_1, ℓ_2 and the ellipse Γ_R. Then, again by (25) and (5),

$$\frac{1}{2\pi} \int_{C_\delta} |K_n(w) g_z(w) dw| \leq \max_{w \in C_\delta} |w-1|^{c-b-1} |w+1|^{b-1} r_t^{-2n-c+1} \int_{C_\delta} |g_z(w)||dw|.$$

Now, on the circle C_δ, that is, for $w = p + |p| s e^{i\theta}$,

$$|g_z(w)| = \left(\frac{|p||z|s}{2} \right)^{-a}$$

and, therefore, since $|p| = \frac{|2-z|}{|z|}$,

$$\int_{C_\delta} |g_z(w)||dw| = \frac{\pi 2^{a+1} |2-z|^{-a+1}}{|z|} s^{-a+1}.$$

In order to optimize the bound with respect to s, we also consider the approximations

$$\max_{w \in C_\delta} |w-1|^{c-b-1} |w+1|^{b-1} \sim |p-1|^{c-b-1} |p+1|^{b-1} = \frac{2^{c-2} |1-z|^{c-b-1}}{|z|^{c-2}}, \quad s \to 0,$$

and

$$r_t \sim r(s) := |p(1-s) + u\sqrt{p^2(1-s)^2 - 1}|, \quad s \to 0. \tag{26}$$

Joining the above results, we finally obtain

$$\frac{1}{2\pi} \int_{C_\delta} |K_n(w) g_z(w) dw| \lesssim C_z r(s)^{-2n-c+1} s^{-a+1}, \tag{27}$$

where

$$C_z = \pi 2^{c+a-1} |1-z|^{c-b-1} |2-z|^{1-a} |z|^{1-c}.$$

Case $a > 1$

By definition (26), $r(s)$ is an increasing function for $s \to 0^+$ and $r(0) = r_p$ (see Figure 1). Therefore, the bound (27) is optimized by looking for the minimum of the function

$$r(s)^{-2n-c+1} s^{-a+1}.$$

Unfortunately, the complexity of $r(s)$ requires further approximations. To this purpose, defining

$$M(s) = p(1-s) + u\sqrt{p^2(1-s)^2 - 1},$$

(cf. (26)), we consider the first order approximation

$$M(0) + sM'(0) = (p + u\sqrt{p^2-1})\left(1 - su\frac{p}{\sqrt{p^2-1}}\right) =: T(s),$$

so that $|T(s)| \sim r(s)$, for $s \to 0$. By using the polar representation

$$\frac{p}{\sqrt{p^2-1}} = \eta e^{i\gamma}, \quad \eta > 0, \tag{28}$$

and defining $k = -2n - c + 1$, the minimum of $|T(s)|^k s^{-a+1}$, for n large enough, is obtained for

$$s_k = \frac{(k+2\overline{a})|\cos\gamma| + \sqrt{(k+2\overline{a})^2\cos^2\gamma - 4\overline{a}(k+\overline{a})}}{2(k+\overline{a})\eta}, \tag{29}$$

where $\overline{a} = -a + 1 < 0$. Observe that $s_k \to 0$, for $n \to +\infty$. Denoting by $\varepsilon_n^{(a,b,c)}(z)$ the error of the method (23), that is,

$$\varepsilon_n^{(a,b,c)}(z) = \left| F(a,b,c,z) - \frac{I_n^{(c-b-1,b-1)}(g_z)}{\gamma_0^{(b,c)}} \right| = \frac{|\mathcal{R}_n(g_z)|}{\gamma_0^{(b,c)}},$$

by (27), we finally have

$$\varepsilon_n^{(a,b,c)}(z) \lesssim \frac{1}{\gamma_0^{(b,c)}} C_z r(s_k)^k s_k^{-a+1}, \quad n \to +\infty. \tag{30}$$

In order to highlight the asymptotic behavior with respect to n, we first note that by (29) we have

$$s_k \sim \frac{-\overline{a}}{\eta|\cos\gamma|(2n + c - 1 - 2\overline{a})},$$

and therefore, after some algebra,

$$\varepsilon_n^{(a,b,c)}(z) \lesssim C_1 e^{-2\ln(r_p)n} n^{a-1}, \quad n \to +\infty,$$

where

$$C_1 = \frac{1}{\gamma_0^{(b,c)}} C_z r_p^{1-c} \left(\frac{a-1}{2\eta|\cos\gamma|}\right)^{1-a} \left| e^{-\frac{\overline{a}up}{\eta|\cos\gamma|\sqrt{p^2-1}}} \right|. \tag{31}$$

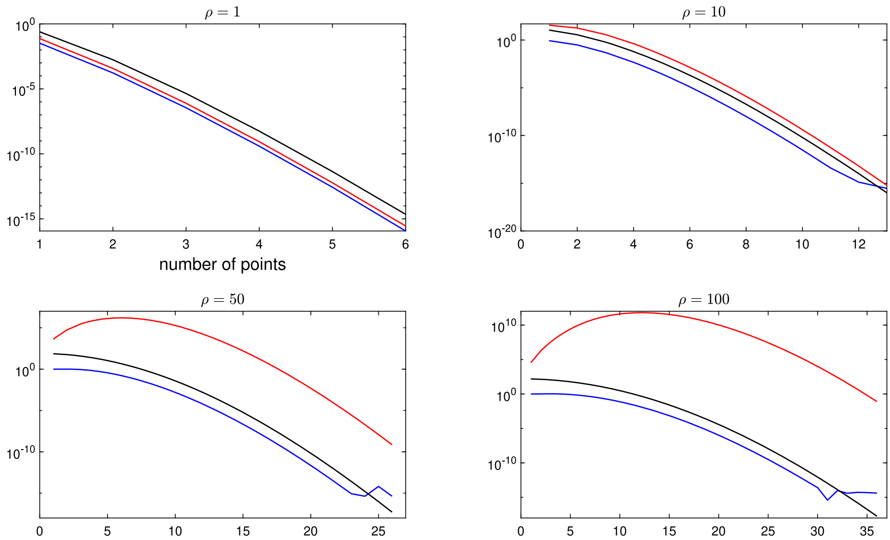

Fig. 2 The relative error for the computation of the confluent hypergeometric function (blue), together with estimate (19) (black) and [3, formula (1.7)] (red), for $\varphi = 0$ and $\rho = 1, 10, 50, 100$. In all cases $a = 1.5$ and $b = 2.5$ (color figure online)

Remark 1 By the definition of γ in (28), we have that $\cos\gamma = 0$ only for $\Re\left(\frac{p}{\sqrt{p^2-1}}\right) = 0$. Since $p = \frac{2}{z} - 1$, this is only possible for $z \in [1, +\infty)$.

Case $a \le 1$

In this situation, since the function

$$r(s)^{-2n-c+1} s^{-a+1},$$

appearing in (27), is monotone decreasing for $s \to 0^+$, the circle C_δ surrounding p can be taken arbitrarily small. Therefore, heuristically we simply use (30) with

$$s_k = -\frac{1}{\eta(k+\overline{a})}, \tag{32}$$

for $-k > \overline{a}$, that is, for n large enough. This choice appears to be fairly good as shown in Figures 8, 9 and 10. Anyway, we remark that for a less than values around -5, the formula based on this choice starts to underestimate the error for large $|z|$. Nevertheless, we also point out that for large negative a the method is extremely fast, so that having at disposal an accurate error estimate is of less importance. With respect to n, the asymptotic behavior is given by

$$\varepsilon_n^{(a,b,c)}(z) \lesssim C_2 e^{-2\ln(r_p)n} n^{a-1}, \quad n \to +\infty, \tag{33}$$

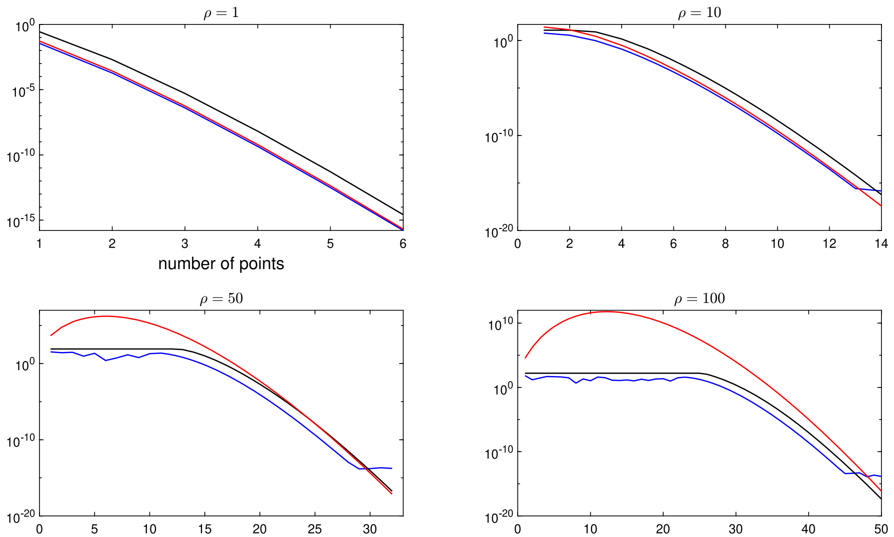

Fig. 3 The relative error for the computation of the confluent hypergeometric function (blue), together with estimate (19) (black) and [3, formula (1.7)] (red), for $\varphi = \frac{\pi}{2}$ and $\rho = 1, 10, 50, 100$. In all cases $a = 1.5$ and $b = 2.5$ (color figure online)

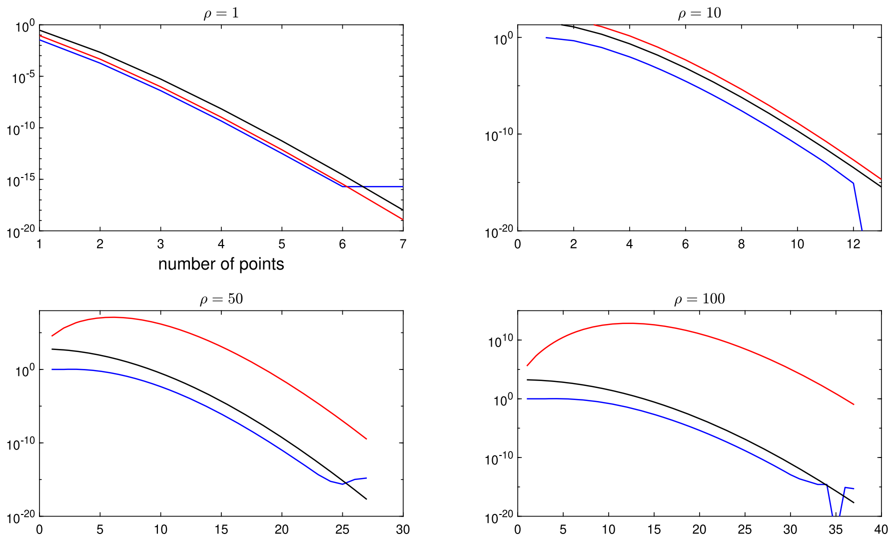

Fig. 4 The relative error for the computation of the confluent hypergeometric function (blue), together with estimate (19) (black) and [3, formula (1.7)] (red), for $\varphi = \pi$ and $\rho = 1, 10, 50, 100$. In all cases $a = 1.5$ and $b = 2.5$ (color figure online)

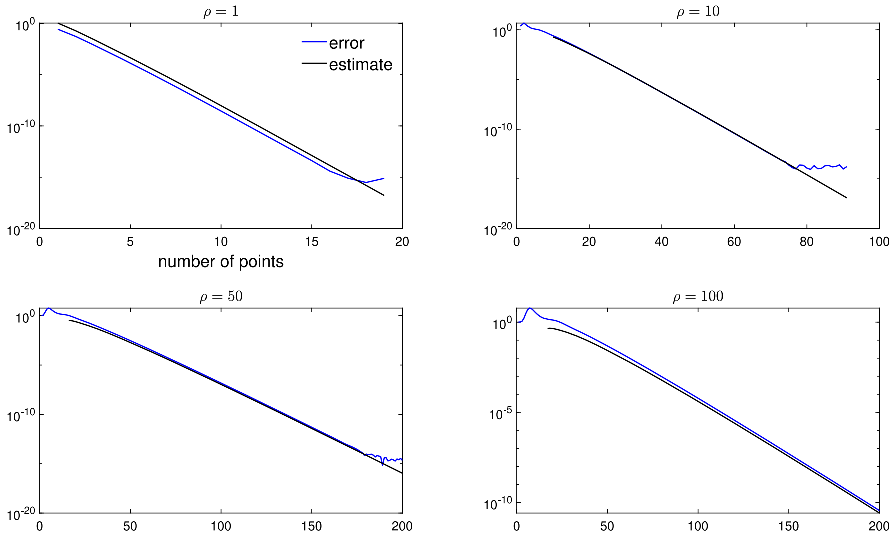

Fig. 5 The relative error for the computation of the Gauss hypergeometric function and bound (30), with s_k as in (29), for $\varphi = \frac{\pi}{4}$ and $\rho = 1, 10, 50, 100$. In all cases $a = 2.5$, $b = 0.5$, $c = 2.7$

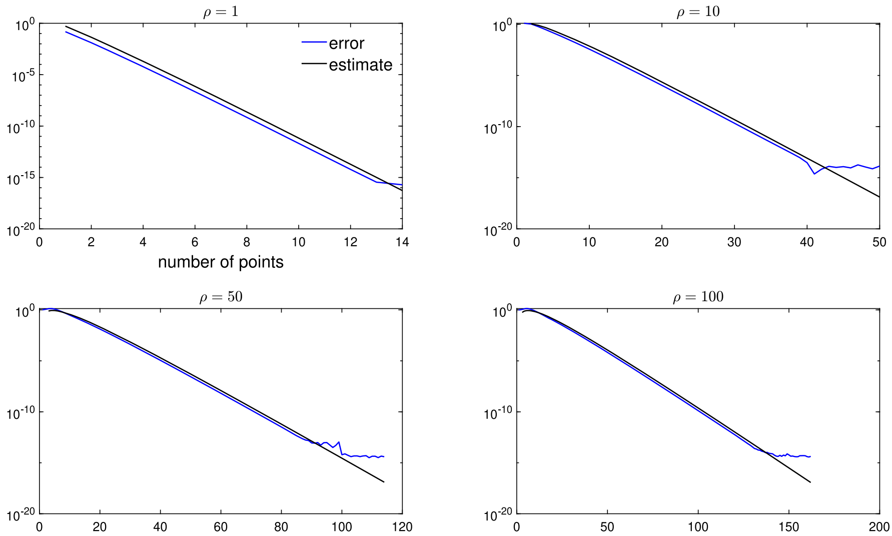

Fig. 6 The relative error for the computation of the Gauss hypergeometric function and bound (30), with s_k as in (29), for $\varphi = \frac{\pi}{2}$ and $\rho = 1, 10, 50, 100$. In all cases $a = 2.5$, $b = 0.5$, $c = 2.7$

where

$$C_2 = \frac{1}{\gamma_0^{(b,c)}} C_z r_p^{1-c} (2\eta)^{a-1} \left| e^{-\frac{up}{\eta\sqrt{p^2-1}}} \right|. \tag{34}$$

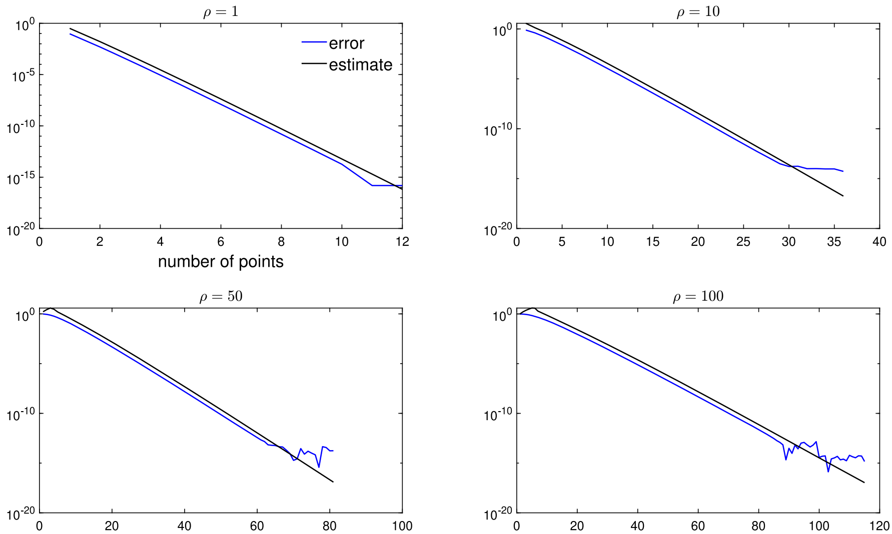

Fig. 7 The relative error for the computation of the Gauss hypergeometric function and bound (30), with s_k as in (29), for $\varphi = \pi$ and $\rho = 1, 10, 50, 100$. In all cases $a = 2.5$, $b = 0.5$, $c = 2.7$

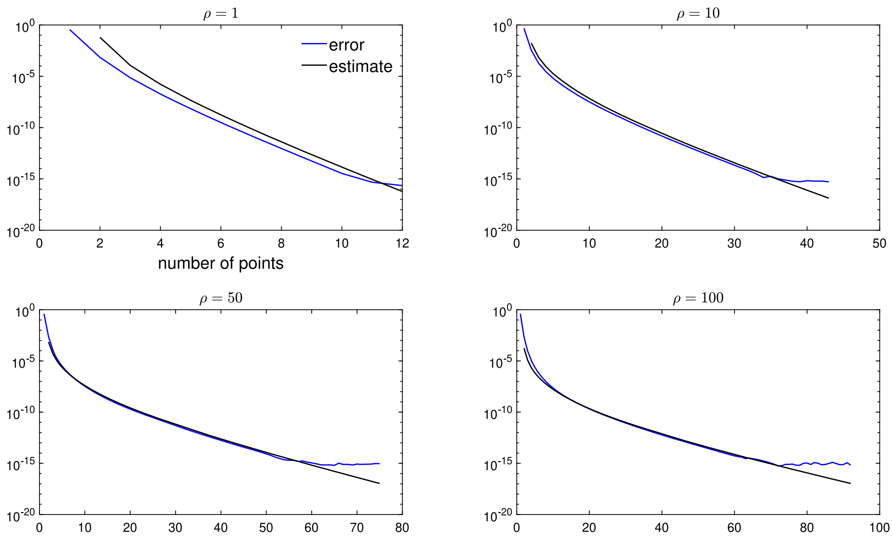

Fig. 8 The relative error for the computation of the Gauss hypergeometric function and bound (30), with s_k as in (32), for $\varphi = \frac{\pi}{4}$ and $\rho = 1, 10, 50, 100$. In all cases $a = -2.7$, $b = 1.3$, $c = 2.7$

Remark 2 For $a = 1$, the function g_z has a simple pole at p. In this situation, by (33) the error decays as $e^{-2 \ln r_p n}$, that is in perfect agreement with the analysis given in [9, formula (2.2)], for analytic functions with simple poles.

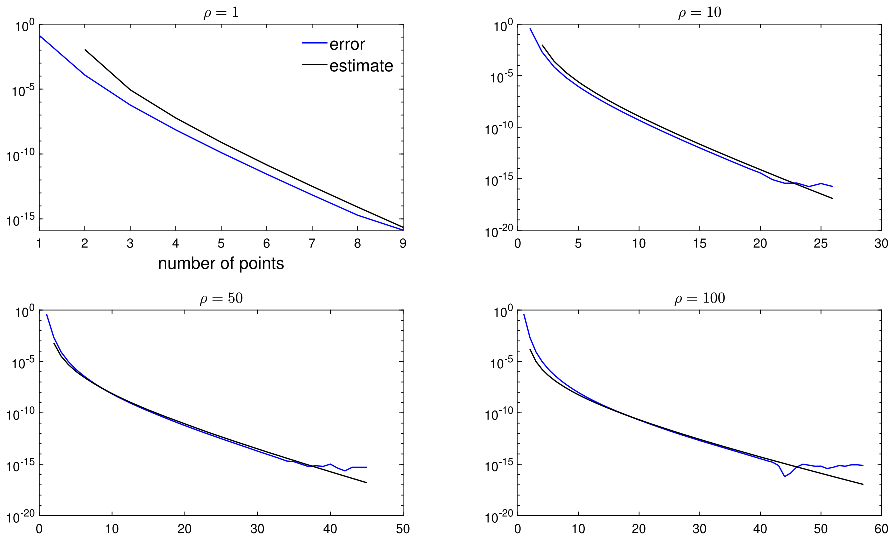

Fig. 9 The relative error for the computation of the Gauss hypergeometric function and bound (30), with s_k as in (32), for $\varphi = \frac{\pi}{2}$ and $\rho = 1, 10, 50, 100$. In all cases $a = -2.7$, $b = 1.3$, $c = 2.7$

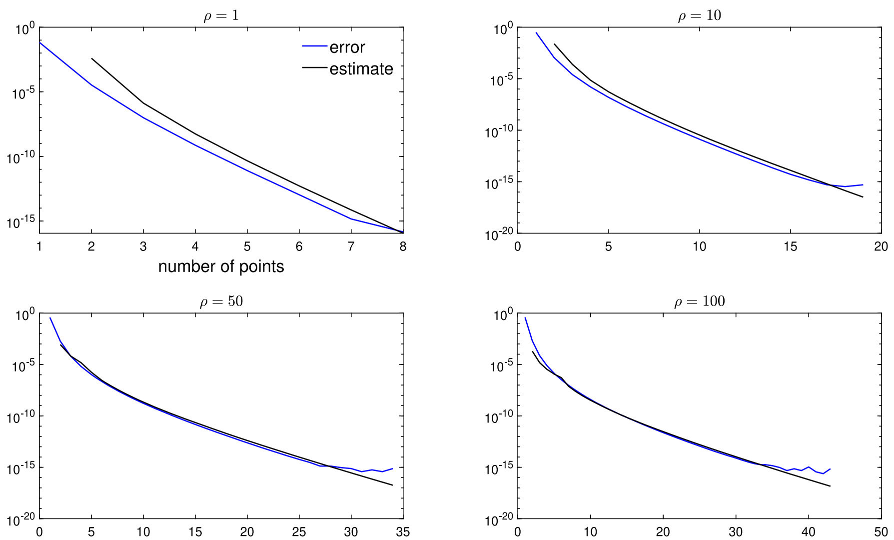

Fig. 10 The relative error for the computation of the Gauss hypergeometric function and bound (30), with s_k as in (32), for $\varphi = \pi$ and $\rho = 1, 10, 50, 100$. In all cases $a = -2.7$, $b = 1.3$, $c = 2.7$

5 Numerical experiments

5.1 Confluent hypergeometric function

In Figures 2, 3 and 4 we consider the relative error arising from the computation of the confluent hypergeometric by means of the Gauss Jacobi rule. We also plot the bound given in formula (19) and the bound [3, (1.7)], both divided by the modulus of the exact solution. In all figures $a = 1.5$, $b = 2.5$, but we consider different phases for the argument z. In particular, $\varphi = 0$ in Figure 2, $\varphi = \frac{\pi}{2}$ in Figure 3 and $\varphi = \pi$ in Figure 4. For each angle, we also consider four different values for the modulus of the argument, that is, $\rho = 1, 10, 50, 100$. What is rather evident from the results is that the two bounds are more or less equivalent and sharp for $|z|$ rather small, independently of $\arg z$. On the other side, for large $|z|$, $z \in \mathbb{R}$, the difference is not negligible and only the bound (19) appears to be accurate.

5.2 Gauss hypergeometric function

In Figures 5, 6, 7, 8, 9 and 10 we consider the relative error for the computation of the Gauss hypergeometric function arising from the Jacobi rule. Figures 5, 6 and 7, that refers to the case of $a > 1$ ($a = 2.5$), contain also the bound (30), with s_k as in (29). In Figures 8, 9 and 10 we have plotted the bound (30), that refers to the case $a \leq 1$ ($a = -2.7$), with s_k as in (32). As before, each figure contains four subplots relative to different values of the modulus of $|z|$, that is, $\rho = 1, 10, 50, 100$. The phases considered are $\varphi = \frac{\pi}{4}, \frac{\pi}{2}, \pi$.

6 Conclusions

In this work we have derived explicit approximations of the error of the Gauss-Jacobi rule for the computation of the confluent and Gauss hypergeometric functions. The analysis is based on the contour integral representation of the remainder term of Gaussian quadrature and on an asymptotic expression for the kernel. We have presented some numerical experiments that confirm the reliability of the bounds, also in relation to existing estimates. Even if we have not introduced new methods for the computation of hypergeometric functions, the strategy developed in Section 4, regarding the proper choice of the contour in the integral representation of the remainder in case of functions analytic in the whole complex plane cut along a line, as far as we know, seems to have never been followed.

Acknowledgements This work was partially supported by GNCS-INdAM and FRA-University of Trieste. The authors are member of the INdAM research group GNCS. Eleonora Denich thanks the University of Trieste for the support, under grant "Programma Regionale (PR) FSE+ 2021/2027 della Regione Autonoma Friuli Venezia Giulia - PPO 2023 - Programma specifico 22/23 - Avviso emanato con decreto n.17895/GRFVG dd.19.04.2023 s.m.i., Linea C) Sportello 2023".

Funding Open access funding provided by Università degli Studi di Trieste within the CRUI-CARE Agreement.

Declarations

Conflicts of Interest The authors declare that there is not conflict of interest.

References

1. Olver, F., Lozier, D., Boisvert, R., Clark, C.: The NIST Handbook of Mathematical Functions. Cambridge University Press, New York, NY (2010)
2. Pearson, J.W., Olver, S., Porter, M.A.: Numerical methods for the computation of the confluent and Gauss hypergeometric functions. Numerical Algorithms **74**(3), 821–866 (2017)
3. Gautschi, W.: Gauss quadrature approximations to hypergeometric and confluent hypergeometric functions. J. Comput. Appl. Math. **139**(1), 173–187 (2002)
4. Davis, P.J., Rabinowitz, P. (eds.): Methods of Numerical Integration. Second edition edn. Academic Press, New York (1984)
5. Gautschi, W.: Orthogonal polynomials, quadrature, and approximation: Computational methods and software (in matlab). In: Marcellán, F., Van Assche, W. (eds.) Orthogonal Polynomials and Special Functions: Computation and Applications, pp. 1–77. Springer, Berlin, Heidelberg (2006)
6. Donaldson, J.D., Elliott, D.: A unified approach to quadrature rules with asymptotic estimates of their remainders. SIAM J. Numer. Anal. **9**(4), 573–602 (1972)
7. Elliott, D.: Uniform asymptotic expansions of the Jacobi polynomials and an associated function. Math. Comput. **25**(114), 309–315 (1971)
8. Gradshteyn, I.S., Ryzhik, I.M.: Tables of Integrals, Series, and Products, 4th edn. Academic Press, New York (1980)
9. Barrett, W.: Convergence properties of gaussian quadrature formulae. Comput. J. **3**(4), 272–277 (1961)